A Theoretical Case Study of Substituent Effects and Microsolvation on the Binding Specificity of Crown Ethers

David Feller,* Mark A. Thompson, and Rick A. Kendall

Environmental Molecular Sciences Laboratory, Pacific Northwest National Laboratory, Richland, Washington 99352

Received: May 5, 1997; In Final Form: July 16, 1997[⊗]

Hartree−Fock and second-order perturbation theory calculations were performed on complexes of a single alkali metal cation and a recently synthesized derivative of 18-crown-6 that locks the crown macrocycle into a D_{3d}-like configuration. Unlike 18-crown-6, which binds K^+ with a 100-fold selectivity over Na^+, the derivative prefers Na^+ by a factor of 4:1. Calculations on a simple $K^+ \leftrightarrow Na^+$ cation exchange reaction indicate a small shift in binding preference in favor of Na^+, but the inherent uncertainty in the theoretical treatment makes an unequivocal conclusion difficult. The effects of two microsolvating waters attached to the cation/s18-crown-6 complex and up through four microsolvating waters bound to 18-crown-6 were considered. The levels of theory used in this study were similar to those previously found to yield binding preferences in qualitative agreement with liquid-phase experimental data. To the best of our knowledge, this work, which involved more than 800 basis functions for several complexes, represents the largest high-level ab initio study of crown ethers yet attempted.

Introduction

The ability of chemical separation agents, such as crown ethers,[1,2] to selectively bind cations of one particular element dispersed in a complex aqueous mixture of chemically similar ions is thought to be dependent on (1) the size of the crown cavity, (2) a subtle balance between cation−ether and cation−water interactions, (3) the presence of substituents on the ligand backbone which alter the crown's electronic environment, and (4) the nature of the electron donor atoms in the ring, e.g., oxygen vs sulfur. In previous theoretical studies of the factors governing crown ether selectivity, we have examined (1) and (2) using ab initio [3−5] and hybrid quantum mechanical/molecular mechanical (QM/MM) molecular dynamics approaches.[6] In the QM/MM studies, quantum mechanical effects were treated with a modified AM1 semiempirical Hamiltonian. Because gas-phase cation−ether interactions are dominated by electrostatics, a monotonic decrease in binding enthalpies is observed with increasing ionic radius along the sequence Li^+, Na^+, ..., Cs^+ (or the corresponding Mg^{2+}, Ca^{2+}, ..., Ra^{2+} sequence) as the distance between the cation and electron donor ether oxygens increases. However, experimentally it is known that ligands such as 18-crown-6 (18c6) in aqueous solution prefers to bind K^+ with a 100-fold selectivity over other alkali metal cations. The disparity between what is predicted in the gas phase and what is observed in solution was resolved in our theoretical studies by adopting the ion exchange reactions

$$K^+{:}18c6 + M^+(H_2O)_n \rightarrow M^+{:}18c6 + K^+(H_2O)_n \quad (M = Li, Na, Rb, Cs) \quad (1)$$

as the basis for judging relative binding preferences. An analogous set of reactions involving Ba^{2+} was used for the alkaline earth dications. Even small number of waters ($n \leq 5$) were sufficient to qualitatively recover the aqueous phase binding trend ($K^+ > Na^+ \sim Rb^+ > Cs^+$), suggesting that any differential entropic effect, which were not accounted for in these studies, was small.

Similar conclusions about the importance of factors (1) and (2) were reached by other investigators. Dang and Kollman[7] and Dang[8] performed molecular mechanics simulations that included the Cl^- counterion. The resulting potentials of mean force and absolute binding energies were in good agreement with experiment, although quantitative agreement with experiment appeared to require improved nonadditive force fields.

Studies are currently underway to examine factors (3) and (4). In the present work we deal with the impact of substituents on the ligand backbone and the influence of water molecules bound to the cation/ether complex as they affect the binding preference of 18c6. The molecular system selected for this work is a recently synthesized derivative of 18c6 that differs from the parent compound due to the presence of six exocyclic rings.[9] These rings effectively lock the primary crown macrocycle into a D_{3d}-like conformation (see Figure 1). Molecular dynamics studies[6,7] of 18c6 have shown it to be quite flexible, sampling many low-lying conformations in aqueous solution. While the C_i conformation of 18c6 is the most frequently observed conformation in crystals, in aqueous phase the molecule is said to be "preorganized" (relative to acyclic polyethers) for binding metal cations because its six oxygens are all pointing toward the center of the crown, in a D_{3d}-like conformation.[10−12] The 18c6 derivative reported by Li and Still[9] is the first to rigidly control the crown backbone. For the sake of brevity, we shall refer to the new crown as s18c6.

In addition to the increased stiffness of the crown ether backbone, two of the exocyclic rings in s18c6 contain a heteroatom (indicated by an X in Figure 1). In the hemiacetal form (X = oxygen), s18c6 has been reported to bind Na^+ preferentially over K^+, whereas 18c6 prefers K^+. Moreover, the work of Li and Still shows s18c6 binds Na^+ and K^+ much more strongly than 18c6. In the hemithiolacetal form (X = sulfur) the original preference for K^+ is restored. Li and Still also examined lithium complexes, but the binding of Li^+ is much weaker than either Na^+ or K^+. In 18c6 the ratio of binding constants (K^+:Na^+) is ∼100:1. In s18c6 the ratio is reversed at ∼1:4.

A goal of the present study is to determine whether the

[⊗] Abstract published in *Advance ACS Abstracts,* September 15, 1997.

S1089-5639(97)01509-0 CCC: $14.00

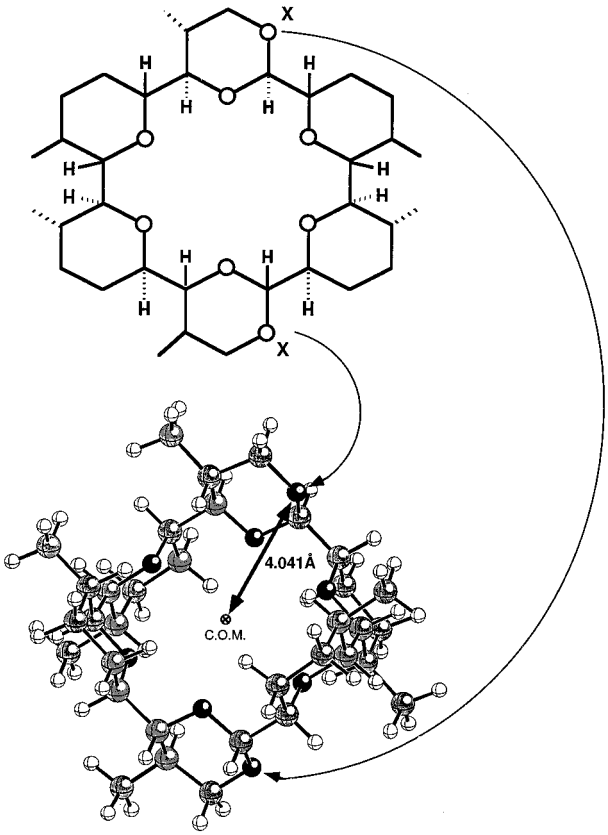

Figure 1. Schematic and ball and stick representations of s18c6. X indicates the positions of the heteroatoms in the exocyclic rings.

cluster-based theoretical treatment shown to correctly model M^+:18c6 binding preferences is capable of likewise describing the novel binding properties of s18c6. If it proves to be adequate, the theoretical model may offer insight into the reasons for the shift in binding preference for Na^+ over K^+ when X = O. Effects due to the increased stiffness of the crown ether backbone in s18c6 are inherently beyond the scope of this work and are being pursued in a separate hybrid QM/MM molecular dynamics studies now in progress.

Procedure

The computational procedure adopted here is the same as that used in our two previous crown ether studies. Geometries for the s18c6 and M^+:s18c6 complexes were initially optimized at the restricted Hartree−Fock (RHF) level with the 3-21G[13] basis set, to obtain normal-mode frequencies and starting geometries for subsequent, larger basis set optimizations. The larger basis set was a composite formed from the 6-31G* basis on H and C and the 6-31+G* basis set on O.[14−16] In the present context we shall use the terms "6-31+G*" and "6-31+G* hybrid" basis set interchangeably. Diffuse functions on oxygen were found to be important for reducing undesirable basis set superposition error (BSSE) which leads to excessively large binding energies. Polarization functions were taken from the earlier work.[3] All six components of the Cartesian d functions were used. The effective core potential (ECP) reported by Hay and Wadt[17] was used for K, and the metal's (3s,3p) electron shell was treated explicitly. Enthalpy corrections to the electronic binding energies were determined with RHF/3-21G frequencies scaled by 0.9.

Except where noted below, all 6-31+G* hybrid basis set calculations were performed with the Gaussian 92[18] and Gaussian 94[19] programs running on local high-speed workstations or the Cray C90 at the U.S. Department of Energy's National Energy Research Scientific Computing Center. The largest chemical systems examined in the present study, M^+:s18c6$(H_2O)_2$, included 105 atoms and 843 basis functions. A single self-consistent-field (SCF) energy evaluation followed by the calculation of first derivatives required 21 central processing unit hours on one node of the C90 or 60 h on a single processor workstation. Processing times were substantially reduced on multiprocessor systems.

A 3-21G geometry for the Na^+:s18c6 complex was obtained with the NWChem program.[20] The 6-31+G* hybrid basis set geometries were optimized with a maximum gradient convergence threshold of ≤ 0.0005 hartree/bohr. The geometry optimization algorithm in Gaussian 94 experienced difficulty handling the complexes with two waters. Several hundred Cartesian optimization steps were required to reach this level of convergence.

Due to hardware and software limitations, we departed from the procedure outlined above for the calculation of the normal-mode frequencies of the two largest complexes. As the basis set size increased beyond 500 functions, the amount of disk storage required for an analytical second derivative calculation became prohibitively large. An alternative algorithm based on numerical differencing of first derivatives would have overcome the disk storage problem at the expense of dramatically increased run times. Consequently, we adopted the STO-3G minimal basis set for obtaining M^+:s18c6$(H_2O)_2$ frequencies. To improve agreement with the 3-21G frequencies, an exponential scale factor[21] was applied to the STO-3G frequencies,

$$\nu_i^{\text{scaled}} = \nu_i s \exp(-\alpha \nu_i) \qquad (2)$$

where $s = 0.9$ and $\alpha = 3.6 \times 10^{-5}$, a value which was chosen to minimize the root-mean-square deviation (σ_{rms}) with 3-21G frequencies for the M^+:s18c6 complexes. For the 291 normal-mode frequencies in K^+:s18c6, exponential scaling reduced σ_{rms} from 210 to 45 cm^{-1}.

Binding energies were corrected for BSSE effects with the full Boys−Bernardi counterpoise (CP) procedure.[22] A recent article by Xantheas[23] reminded readers of the importance of using fragment geometries taken from the optimized complex when computing this correction. In the present work, as well as in all of our previous work, CP corrections were computed with the so-called "relaxed" fragment geometries. At the RHF level of theory the size of the CP correction falls in the range 2−5 kcal/mol for the complexes studied here.

Second-order Møller−Plesset perturbation theory (MP2) was used to estimate the effect of electron correlation on the cation−crown binding energies. We were unable to compute the MP2 counterpoise correction for the alkali cation−s18c6 complexes with Gaussian on our local compute servers because of an extended period of hardware instability. MP2 calculations with Gaussian are nonrestartable, and both of the M^+(ghost):crown runs required an estimated 11 days of time on two processors. Instead, both of these calculations were performed on an IBM SP/2 with the beta 2.1 version of NWChem. As an example of the type of speedup possible with massively parallel hardware and software, the MP2 calculation on Na^+:s18c6 took 115 wall clock hours on two nodes of an SGI PowerChallenge with Gaussian 94 and just 13 wall clock hours on 135 processors of the SP/2 with NWChem.

Previous attempts to calibrate this basis set and level of theory against larger basis sets and more extensive correlation recovery (i.e., fourth order of perturbation theory and coupled cluster theory) suggest that MP2/6-31+G*(CP) binding energies are typically within several kcal/mol of the best estimates available.[24,25] Due to the size of the s18c6 calculations, it is currently

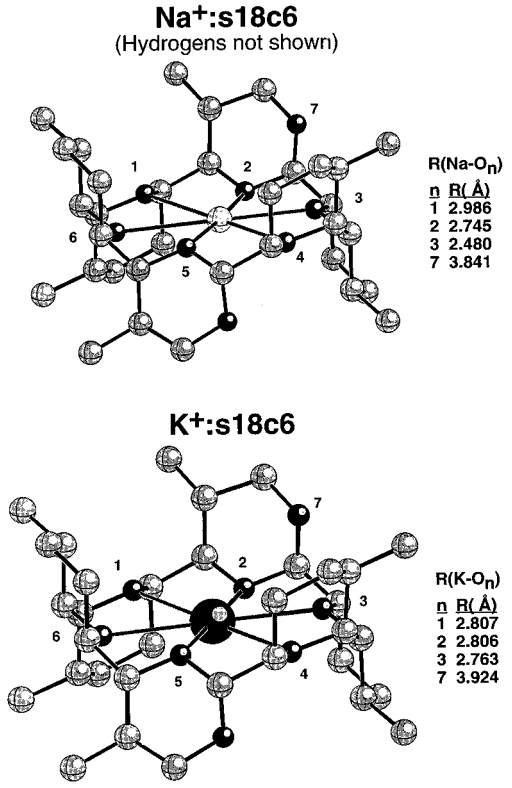

Figure 2. RHF/6-31+G* hybrid optimized structures for Na^+:s18c6 and K^+:s18c6. Hydrogens are not shown in order to emphasize the carbon/oxygen framework.

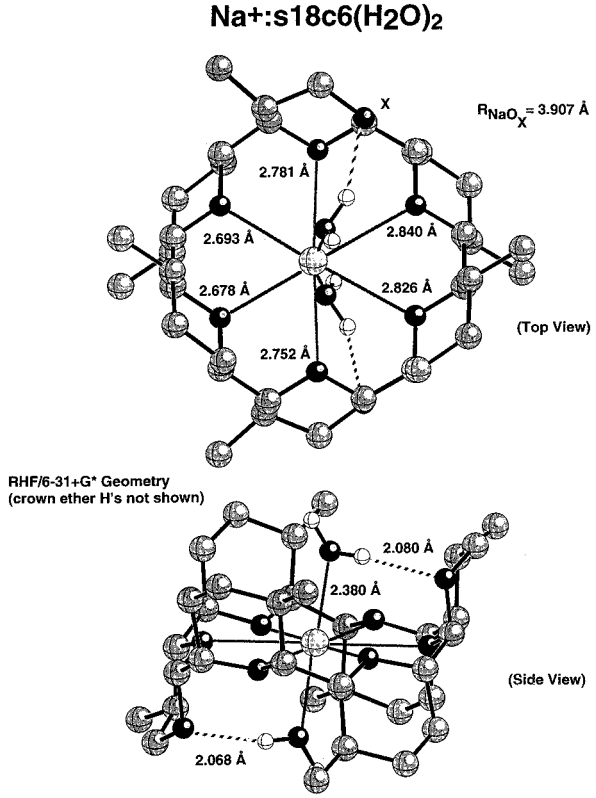

Figure 3. RHF/6-31+G* hybrid optimized structures for Na^+:s18c6-$(H_2O)_2$ with hydrogens not shown.

impossible for us to employ larger basis sets in an attempt to judge the degree of convergence in our findings.

s18c6, M^+:s18c6, and M^+:s18c6$(H_2O)_2$ Geometries

The RHF/6-31+G* optimized geometry of bare s18c6 has been reported previously.[26] An analysis of this structure reveals only minor differences in the macrocycle, compared to 18c6, resulting from the six exocyclic rings. The transannular O−O cross ring distance has decreased slightly (∼0.1 Å) to 5.70 Å, and the OCCO dihedral angles have decreased by 5° to 70.6°. All CC and CO bond lengths are within 0.01 Å of the corresponding bond lengths in 18c6. As seen in Figure 1, the exocyclic rings form a C_2 symmetry sleeve in which the crown macrocycle is embedded. The distance from the center of mass to one of the exocyclic oxygens is 4.041 Å.

Optimized structures for the Na^+:s18c6 and K^+:s18c6 complexes are displayed in Figure 2. Metal−oxygen distances to the macrocyclic ether oxygens (M^+-O_{macro}) are ∼0.02 Å longer than the corresponding values in the M^+:18c6 complexes. The added stiffness caused by the exocyclic rings prevents the crown macrocycle from contracting around the metal cation, as it does in the parent compound. Nonetheless, the presence of the cation in the s18c6 complexes produces a significant distortion in the exocyclic oxygen rings, pulling portions of the rings inward toward the cation by 0.20 Å (Na^+) or 0.12 Å (K^+).

In the Na^+:s18c6 complex, the crown macrocycle no longer displays D_{3d} symmetry, with Na−O distances varying by as much as ±0.5 Å. Our previous study of Na^+:18c6 identified two nearly degenerate, low-lying conformations. One displayed D_{3d} symmetry, with each of the six ether oxygens lying roughly in a plane. In the other conformation, of C_1 symmetry, the crown folded in order to wrap around the relatively small sodium cation. This yielded a shorter average Na−O distance but required a large penalty in terms of the distortion energy. The present Na^+:s18c6 structure qualitatively appears to be a composite of the D_{3d} and C_1 Na^+:18c6 structures.

The distance between the central cation and the two exocyclic oxygens (M^+-O_{exo}) is much larger than the distance to the six oxygens in the macrocycle. For example, in the Na^+:s18c6 complex the longest Na^+-O_{macro} distance is 2.99 Å, compared to a Na^+-O_{exo} distance of 3.84 Å. However, due to the slow $1/r$ falloff with distance of the electrostatic interaction, the M^+-O_{exo} interaction contribution to the stability of the complex is still appreciable. As a rough guide to the magnitude of the M^+-O_{exo} interaction, we performed a calculation on Na^+ and a single water molecule with an Na^+-O distance of 2.99 Å. $\Delta E_{binding}$ is 18 kcal/mol, including the CP correction, which falls off by only 39% (to 11 kcal/mol) when the Na^+-O distance is increased to 3.84 Å.

No experimental structural information is available for the bare s18c6 or its complexes with Na^+ and K^+. However, Li and Still[9] reported a crystal structure for Na^+:s18c6$(H_2O)_2$ with a thiocyanate counterion. The two waters cap opposite ends of the s18c6 sleeve, forming hydrogen bonds with the exocyclic oxygens (see Figure 3). The agreement of the RHF/6-31G* hybrid geometry with the crystal structure is generally good. Fortuitously, the average Na^+-O_{macro} distances are in exact agreement at 2.76 Å. However, individual Na^+-O distances vary between theory and experiment by as much as 0.1 Å. RHF theory predicts a longer Na^+-O_{water} distance (2.382 Å) than is observed in the X-ray structure (2.313 Å). In the presence of the two additional waters, the distance between Na^+ and the exocyclic oxygens increases by 0.06 Å.

Binding Enthalpies

The Na^+:s18c6 and K^+:s18c6 counterpoise corrected, electronic binding energies (ΔE) and binding enthalpies at 298 K (ΔH^{298}) are listed in Table 1, along with the corresponding total energies. Compared to the binding energies for the parent

TABLE 1: Results for S18c Complexes Obtained with the 6-31+G* Hybrid Basis Set[a]

system	level	E (hartrees)	no. of funct	E_{ZPT}	ΔE(CP)[b]	ΔH^{298}(CP)
s18c6	RHF	−1919.0421	774	533.1		
	MP2	−1924.9434				
Na^+:s18c6	RHF	−2080.8508	797	535.0	−91.1	−89.5
	MP2	−2086.7706			−93.0	−91.4
K^+:s18c6	RHF	−1946.8705	789	534.8	−75.8	−74.5
	MP2	−1952.8625			−81.5	−80.2
Na^+:s18c6$(H_2O)_2$	RHF	−2232.9232	843	574.4	−109.0	−102.9
K^+:s18c6$(H_2O)_2$	RHF	−2098.9347	835	574.3	−90.3	−84.5

[a] Total energies are given in hartrees. Zero-point vibrational energies and energy differences are given in kcal/mol. The vibrational energies were obtained from scaled RHF/3-21G frequencies, except for the complexes with two waters. The latter were obtained by an exponential scaling of STO-3G frequencies, as explained in the text. [b] ΔE represents the binding energy for the process $M^+ + s18c6 \rightarrow M^+$:s18c6 or $M^+ + s18c6 + 2H_2O \rightarrow M^+$:s18c6$(H_2O)_2$. The RHF binding energies for the M^+:s18c6$(H_2O)_2 \rightarrow M^+ + s18c6(H_2O)_2$ processes were −100.1 kcal/mol (Na^+) and −81.4 kcal/mol (K^+).

compound, obtained at the same level of theory, the present values are 15−20% stronger due to the presence of the two exocyclic oxygens. At the RHF level the sodium ΔE values (in kcal/mol), corrected for BSSE, are −91.1 (s18c6) vs −78.8 (18c6) and for potassium −75.8 (s18c6) vs −68.1 (18c6), in qualitative agreement with the experimental observation that s18c6 is significantly more ionophoric that 18c6. Enthalpy changes parallel the changes in ΔE.

A Mulliken population analysis with the 3-21G or 6-31+G* hybrid basis sets shows the exocyclic ether oxygens bearing a partial charge of −0.66 *e*. The charges on the macrocyclic oxygens (−0.55 *e*) are essentially identical with the values in the parent 18c6. Mulliken charges further indicate substantial negative charges on the carbons comprising the exocyclic rings, in the range −0.3 to −0.4 *e*. However, the latter charges are largely canceled by the positive charges on the hydrogens, leaving each CH_2 fragment with a small overall positive charge. Other than the addition of the exocyclic oxygens, the only significant change indicated by the Mulliken populations is the positive charge gained by the two macrocyclic carbons that are bonded to exocyclic oxygens. In 18c6 they were essentially neutral, while in s18c6 they bear charges of +0.5 *e*, which increases to +0.7 *e* if the attached hydrogen's charge is added.

Since Mulliken partial charges are known to sometimes change considerably from one basis set to another, we also analyzed the RHF wave functions with the natural population analysis/natural bond order (NPA/NBO) method of Weinhold and co-workers,[27,28] which has been shown to be much less sensitive to the choice of basis set. NPA/NBO charges on the macrocyclic oxygens in s18c6 were slightly more negative than Mulliken charges, −0.65 *e* (NBO) vs −0.52 *e* (Mulliken), and the exocyclic oxygens have essentially identical charges.

To simulate the enthalpy change for the $K^+ \leftrightarrow Na^+$ cation exchange reaction (1) in solution, we have extended our earlier work,[3] which included $M^+(H_2O)_n$ complexes only through $n = 4$. The 6-31+G* basis set total binding energies for $M^+(H_2O)_n$, $n = 5$ and 6, were obtained from the literature.[29] These were augmented with new calculations for the $n = 7$, 8, and 9 complexes. The lowest energy structures, shown in Figure 5, place the seventh water in the primary solvation shell for K^+ and the secondary shell for Na^+. We were unable to locate a minimum in which all seven waters were directly coordinated to Na^+. The same is true of the $n = 8$ cluster. With nine waters potassium's first solvation shell is filled, and the ninth water starts the second solvation shell.

Although the number of $M^+(H_2O)_n$ conformations increases rapidly with *n*, variations in energy among the lowest few structures is normally small.[29,24] Thus, while there is no guarantee that the four structures in Figure 5 represent global minima, the error introduced in the calculation of ΔH for the exchange reaction would likely be small. The total binding enthalpy for the cation/water clusters in Figure 5 is defined as ΔH for the reaction $M^+(H_2O)_n \rightarrow M^+ + n(H_2O)$. RHF and MP2 values of the binding energy and binding enthalpies are presented in Table 2.

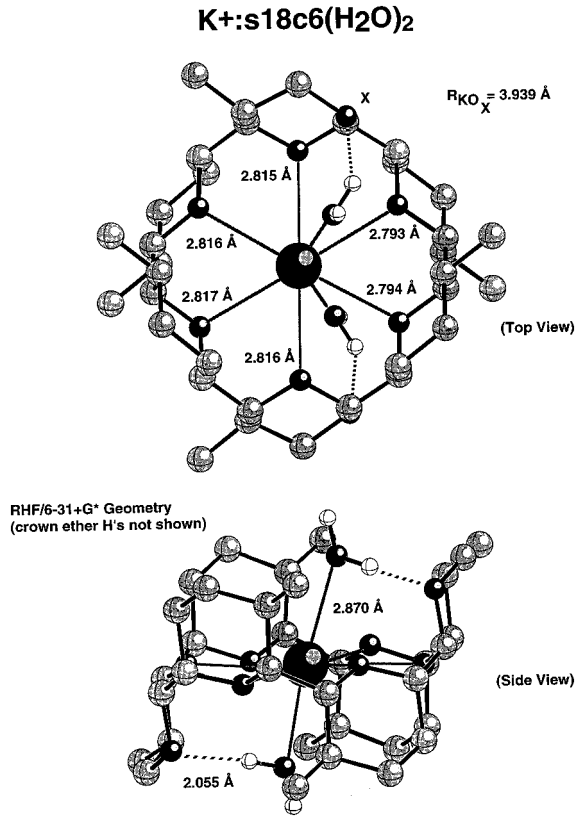

Figure 4. RHF/6-31+G* hybrid optimized structures for K^+:s18c6-$(H_2O)_2$ with hydrogens not shown.

Figure 6 shows the variation in ΔH for the $K^+ \leftrightarrow Na^+$ exchange reaction as a function of *n*, the number of waters included in the $M^+(H_2O)_n$ clusters with K^+ arbitrarily defined to be the zero of enthalpy. Negative values of ΔH correspond to a binding preference for Na^+ over K^+. As noted previously,[3] the relative binding preferences change very rapidly as *n* increases, with qualitative agreement between the gas-phase cluster calculations and aqueous-phase experiments reached with as few as 4−5 waters. For $n \geq 6$, fluctuations are observed in the enthalpy curves as the first solvation shell of the $Na^+(H_2O)_n$ clusters is filled, but the larger potassium cation is still filling in its first shell. Because the seventh and eighth waters in the potassium clusters are able to bind directly to the cation, as well as participate in multiple hydrogen bonds, the right-hand side of eq 1 is temporarily favored. As noted earlier, continuing

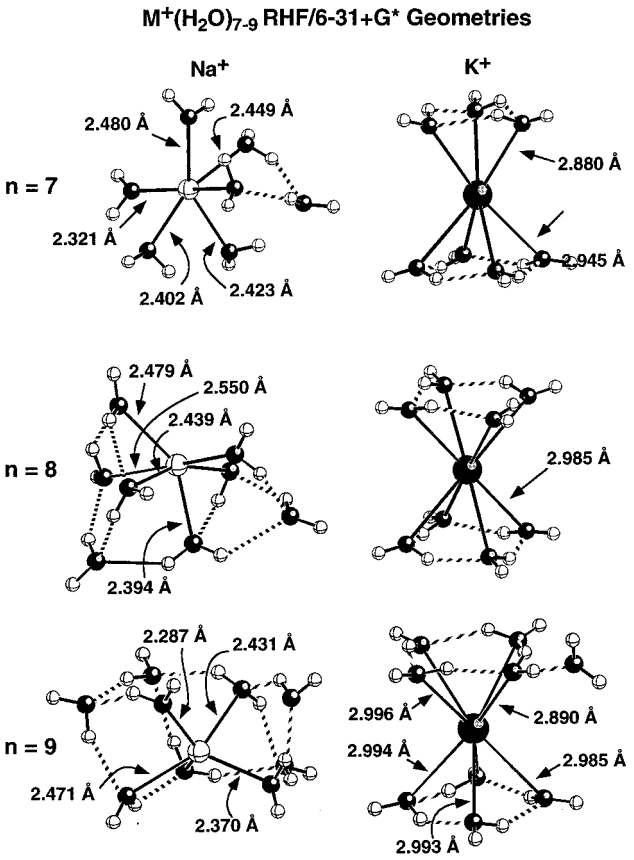

Figure 5. Lowest energy RHF/6-31+G* hybrid optimized structures for $Na^+(H_2O)_n$ and $K^+(H_2O)_n$, $n = 7-9$.

TABLE 2: Counterpoise-Corrected Total Binding Energies and Enthalpies for $M^+(H_2O)_n$, $n = 7-9$, Obtained with the 6-31+G* Hybrid Basis Set[a]

n	sym	level	geom	*E* (hartrees)	ΔE(CP)[b]	ΔH^{298}(CP)
			$Na^+(H_2O)_n$			
7	C_1	RHF	opt RHF	−693.9762	−112.5	−101.8
	C_1	MP2	opt RHF	−695.3430	−118.5	−107.8
8	C_1	RHF	opt RHF	−770.0101	−119.6	−106.8
	C_1	MP2	opt RHF	−771.5749	−126.1	−113.2
9	C_1	RHF	opt RHF	−846.0472	−129.3	−112.5
	C_1	MP2	opt RHF	−847.8092	−138.2	−120.8
			$K^+(H_2O)_n$			
7	C_1[b]	RHF/ECP	opt RHF	−559.9853	−92.4	−81.6
	C_1[b]	MP2/ECP	opt RHF	−561.4206	−100.1	−89.3
8	S_4	RHF/ECP	opt RHF	−636.0215	−102.2	−89.6
	S_4	MP2/ECP	opt RHF	−637.6532	−111.5	−98.8
9	C_1	RHF/ECP	opt RHF	−712.0545	−110.6	−93.9
	C_1	MP2/ECP	opt RHF	−713.8805	−120.8	−104.1

[a] Total energies are in hartrees. Binding energies and enthalpies are in kcal/mol. The sodium 1s electrons were treated as core. The potassium (1s,2s,2p) were represented by an effective core potential. [b] The K/O framework has approximate C_2 symmetry.

this sequence through $n = 9$ begins to fill in the second solvation shell around K^+, and the curvature of the ΔH vs n lines in Figure 6 changes sign for both M^+:18c6 and M^+:s18c6 curves, displaying a shift in favor of K^+. This results from the stronger incremental binding energy of a water molecule in $Na^+(H_2O)_n$'s second solvation shell compared to potassium. Overall, the s18c6 MP2 curve, without microsolvating waters, is shifted in favor of Na^+ by 4.5 kcal/mol, relative to the 18c6 curve.

MP2 correlation corrections to the M^+:s18c6 binding energies were obtained at the optimal RHF geometries. As was the case with 18c6, correlation effects strengthen the cation−ligand binding by 3−6 kcal/mol, but the *differential* effects on the two

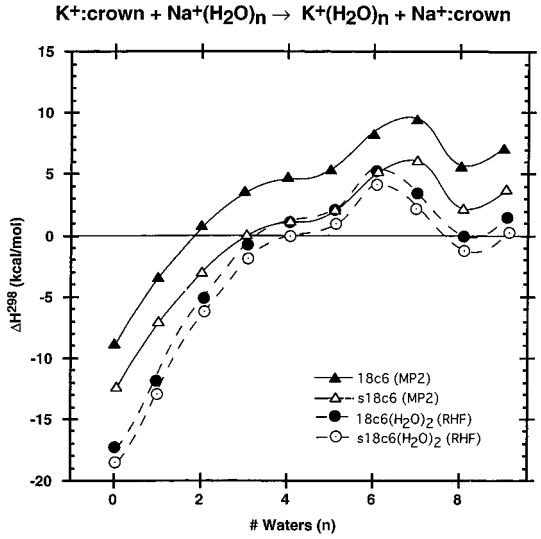

Figure 6. Enthalpy change for the cation exchange reactions K^+:crown + $Na^+(H_2O)_n \rightarrow Na^+$:crown + $K^+(H_2O)_n$ and K^+:crown$(H_2O)_2$ + $Na^+(H_2O)_n \rightarrow Na^+$:crown $(H_2O)_2$ + $K^+(H_2O)_n$ obtained with the 6-31+G* hybrid basis set.

cations are much smaller. ΔH for the $K^+ \leftrightarrow Na^+$ cation exchange reaction increases by 0.9 kcal/mol at the MP2 level.

As seen in Table 1, the presence of the two capping waters in the region of space between the central cation and the exocyclic oxygens results in a strengthening of the metal−ligand bond for both Na^+ and K^+, although the complex containing the former cation benefits somewhat more. This results in a 3.5 kcal/mol shift in ΔH for the exchange reaction in favor of sodium.

To more directly compare s18c6 and the parent 18c6 compound, two additional sets of calculations were performed on microsolvated forms of 18c6. The first of these calculations were carried out on the M^+:18c6$(H_2O)_2$, M = Na^+ and K^+, complexes, whose RHF/6-31+G* optimized geometries are shown in Figure 7. Without the exocyclic oxygens to help anchor the capping waters, the average M^+-O distances to the waters are 0.02−0.06 Å longer than in M^+:s18c6$(H_2O)_2$. The added waters form strained hydrogen bonds to two of the macrocyclic oxygens, causing the corresponding M^+-O_{macro} distances to both lengthen. Similar behavior has been noted for the M^+:18c6$(H_2O)_2$ complexes with the other alkali cations.[5] In the case of the Na^+:18c6$(H_2O)_2$ complex, the distortion in the previously D_{3d} symmetry macrocycle is particularly noticeable.

The addition of two capping waters to M^+:18c6 results in a shift in the energetics of the cation exchange reaction enthalpies by 6.6 kcal/mol at the RHF level (4.6 kcal/mol at the MP2 level) toward the Na^+:crown side of the equation (see Figure 6). Up through nine cation waters of solvation, i.e., considering $M^+(H_2O)_n$, $n \leq 9$, potassium is still preferred over sodium, but the magnitude of the binding preference has been significantly cut. Fluctuations of the type observed in Figure 6 suggest that it will be difficult to draw more definitive conclusion based on these types of cluster calculations. On the basis of this comparison, we find a small (1.5 kcal/mol) shift in the binding affinity in favor of sodium for s18c6. We were unable to determine the MP2 correction to this shift due to the size of the calculations.

A second set of microsolvation calculations on 18c6 were performed with a total of four microsolvating waters (two on the top and two on the bottom). These complexes are shown in Figure 8. In terms of the numbers of nonmacrocycle oxygens,

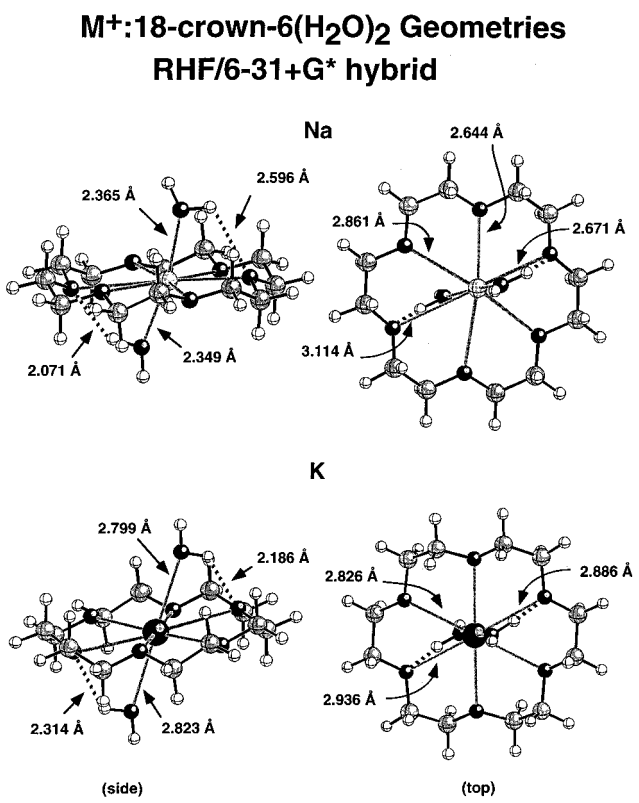

Figure 7. RHF/6-31+G* hybrid optimized geometries for M^+:18c6-$(H_2O)_2$, M = Na and K.

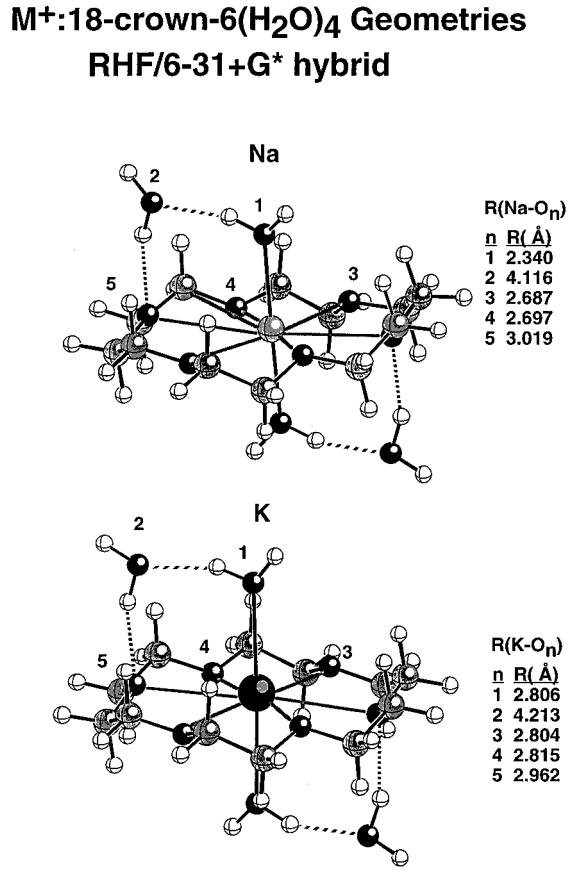

Figure 8. RHF/6-31+G* hybrid optimized geometries for M^+:18c6-$(H_2O)_4$, M = Na and K.

M^+:18c6$(H_2O)_4$ and M^+:s18c6$(H_2O)_2$ complexes are equivalent, although they obviously differ somewhat in several structural features. The distance between the metal cation and the directly bonded water has decreased by ~0.05 Å in the M^+:18c6$(H_2O)_4$ complexes relative to M^+:s18c6$(H_2O)_2$. On the other hand, the distance between the metal and the oxygen labeled O(2) in Figure 8 is ~0.24 Å longer than the M^+-O_{exo} distance in the M^+:s18c6$(H_2O)_2$ complexes. These effects appear to largely cancel, with the net result that M^+:18c6$(H_2O)_4$ and M^+:s18c6-$(H_2O)_2$ complexes bind sodium with roughly equal strength. Thus, if one were to use M^+:18c6$(H_2O)_4$ as the basis for deciding whether s18c6 exhibited a stronger binding preference for Na^+, one would be forced to conclude that no such effect existed.

Conclusion

Ab initio Hartree−Fock theory was used to determine the structures of four complexes comprised of a single alkali metal cation (Na^+ or K^+) and a recently synthesized derivative of 18c6 that has been reported to display novel binding preferences. The enthalpies of reaction for a simple $K^+ \leftrightarrow Na^+$ cation exchange reaction were used as the basis for determining binding preferences. The present work accounted for (1) electron correlation effects, (2) basis set superposition errors, and (3) microsolvating the 18c6 ligand in order to place the parent compound in an enviroment that was as similar as possible to the M^+:s18c6$(H_2O)_2$ environment.

The validity of our cluster approach to modeling condensed phase enthalpies of exchange depends upon how well the clusters mirror the essential physics of the important configurations found in the fully solvated system. We cannot, in general, predict a priori the most important clusters, or even representative clusters, without resorting to results of experiment or molecular simulations which would give us structural information, from which we could build our cluster models. For example, in our QM/MM simulation of K^+:18c6, we observed that the cation coordinated two solvent waters, on average, based on a radial distribution function analysis.[6] Thus, we conclude that the most valid microsolvated M^+:18c6 cluster to examine would be M^+:18c6$(H_2O)_2$; clusters with more waters could generate artifically important minina that may skew the analysis. Similarly, on the basis of the X-ray structure of Li and Still,[9] we might also conclude that M^+:s18c6$(H_2O)_2$ is the appropriate microsolvated cluster to examine.

Following this line of reasoning, our results in Figure 6 indicate that, all else being equal, s18c6 shows an enhanced selectivity for Na^+ over K^+ of roughly 1.5 kcal/mol based on comparing the M^+:18c6$(H_2O)_2$ and M^+:s18c6$(H_2O)_2$ curves. However, we note that tests of the accuracy of the present theoretical approach against larger basis set calculations that incorporate higher levels of correlation recovery suggest conservative error bars of several kcal/mol for 6-31+G* binding energies. Thus, an unequivocal conclusion based on the present work is not possible. Finally, because differential entropic effects are very difficult to compute accurately for large cation/ligand complexes, further studies, involving molecular dynamics simulations, may be needed to rule out such effects as a major contributor to the preference of s18c6 for sodium.

Acknowledgment. D.F. thanks Dr. Jeff Nichols for his help in running the NWChem calculations. As noted in the text, several large MP2 counterpoise calculations were run with the beta 2.1 version of NWChem on an IBM SP/2 which is part of the Molecular Science Computing Facility in the Environmental Molecular Sciences Laboratory at the Pacific Northwest National Laboratory. This research was supported by the U.S. Department of Energy under Contract DE-AC06-76RLO 1830 (Division of Chemical Sciences, Office of Basic Energy Sciences). The

Pacific Northwest National Laboratory is operated by Battelle Memorial Institute. We acknowledge helpful discussions with Prof. Eric Glendening of Indiana State University. We also thank the Scientific Computing Staff, Office of Energy Research, U.S. Department of Energy, for a grant of computer time at the National Energy Research Scientific Computing Center (Berkeley, CA). In particular, we thank Ms. Betsy Foote, Mr. Michael Wilson, and Mr. Alan Riddle, NERSC staff members, who assisted us in the use of special parallel computing facilities at NERSC during the course of this work.

References and Notes

(1) Pedersen, C. J. *J. Am. Chem. Soc.* **1967**, *89*, 2495.
(2) Pedersen, C. J. *J. Am. Chem. Soc.* **1967**, *89*, 7017.
(3) Glendening, E. D.; Feller, D.; Thompson, M. A. *J. Am. Chem. Soc.* **1994**, *116*, 10657.
(4) Glendening, E. D.; Feller, D. *J. Am. Chem. Soc.* **1996**, *118*, 6052.
(5) Feller, D. *J. Phys. Chem. A* **1997**, *101*, 2723.
(6) Thompson, M. A.; Glendening, E. D.; Feller, D. *J. Phys. Chem.* **1994**, *98*, 10465.
(7) Dang, L. X.; Kollman, P. A. *J. Phys. Chem.* **1995**, *99*, 55.
(8) Dang, L. X. *J. Am. Chem. Soc.* **1995**, *117*, 6954.
(9) Li, G.; Still, W. C. *J. Am. Chem. Soc.* **1993**, *115*, 3804.
(10) Ha, Y. L.; Chakraborty, A. K. *J. Phys. Chem.* **1991**, *95*, 10781.
(11) Straatsma, T. P.; McCammon, J. A. *J. Chem. Phys.* **1989**, *91*, 3631.
(12) Dang, L. X.; Kollman, P. A. *J. Am. Chem. Soc.* **1991**, *112*, 5716.
(13) Binkley, J. S.; Pople, J. A.; Hehre, W. J. *J. Am. Chem. Soc.* **1980**, *102*, 939.
(14) Hehre, W. J.; Ditchfield, R.; Pople, J. A. *J. Chem. Phys.* **1972**, *56*, 2257.
(15) Clark, T.; Chandrasekhar, J.; Spitznagel, G. W.; Schleyer, P. v. R. *J. Comput. Chem.* **1983**, *4*, 294.
(16) Hariharan, P. C.; Pople, J. A. *Theor. Chim. Acta* **1973**, *28*, 213.
(17) Hay, P. J.; Wadt, W. R. *J. Chem. Phys.* **1985**, *82*, 299.
(18) Frisch, M. J.; Trucks, G. W.; Head-Gordon, M.; Gill, P. M. W.; Wong, M. W.; Foresman, J. B.; Johnson, B. G.; Schlegel, H. B.; Robb, M. A.; Replogle, E. S.; Gomperts, R.; Andres, J. L.; Raghavachari, K.; Binkley, J. S.; C. Gonzalez; Martin, R. L.; Fox, D. J.; Defrees, D. J.; Baker, J.; Stewart, J. J. P.; Pople, J. A. *Gaussian 92*; Gaussian, Inc.: Pittsburgh, PA, 1992.
(19) Frisch, M. J.; Trucks, G. W.; Schlegel, H. B.; Gill, P. M. W.; Johnson, B. G.; Robb, M. A.; Cheeseman, J. R.; Keith, T. A.; Petersson, G. A.; Montgomery, J. A.; Raghavachari, K.; Al-Laham, M. A.; Zakrzewski, V. G.; Ortiz, J. V.; Foresman, J. B.; Cioslowski, J.; Stefanov, B. B.; Nanayakkara, A.; Challacombe, M.; Peng, C. Y.; Ayala, P. Y.; Chen, W.; Wong, M. W.; Andreas, J. L.; Replogle, E. S.; Gomperts, R.; Martin, R. L.; Fox, D. J.; Binkley, J. S.; Defrees, D. J.; Baker, J.; Stewart, J. J. P.; Head-Gordon, M.; Gonzalez, C.; Pople, J. A. *Gaussian 94*, D.3; Gaussian, Inc.: Pittsburgh, PA, 1996.
(20) Group, H. P. C. C. NWChem, Pacific Northwest National Laboratory, Richland, WA 99352, 1996.
(21) Kim, J.; Lee, S.; Cho, S. J.; Mhin, B. J.; Kim, K. *J. Chem. Phys.* **1995**, *102*, 839.
(22) Boys, S. F.; Bernardi, F. *Mol. Phys.* **1970**, *19*, 553.
(23) Xantheas, S. S. *J. Chem. Phys.* **1996**, *104*, 8821.
(24) Feller, D.; Glendening, E. D.; Woon, D. E.; Feyereisen, M. W. *J. Chem. Phys.* **1995**, *103*, 3526.
(25) Feller, D.; Aprà, E.; Nichols, J. A.; Bernholdt, D. E. *J. Phys. Chem.* **1996**, *100*, 1940.
(26) Thompson, M. A. *Int. J. Quantum Chem.* **1996**, *60*, 1133.
(27) Reed, A. E.; Weinstock, R. B.; Weinhold, F. *J. Chem. Phys.* **1985**, *83*, 735.
(28) Glendening, E. D.; Badenhoop, J. K.; Reed, A. E.; Carpenter, J. E.; Weinhold, F. *NBO version 4.0*; Theoretical Chemistry Institute, University of Wisconsin: Madison, 1994.
(29) Glendening, E. D.; Feller, D. *J. Phys. Chem.* **1995**, *99*, 3060.